

CONF 470706-22

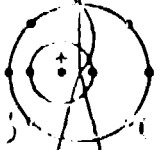
TITLE: SOUND VELOCITY ON SiO<sub>2</sub> HUGONIOTS

AUTHOR(S): J. A. Morgan and J. N. Fritz

SUBMITTED TO: 6th AIRAPT International High Pressure Conference, Applications and Techniques University of Colorado, Boulder, CO July 25-29, 1977

By acceptance of this article for publication, the publisher recognizes the Government's (license) rights in any copyright and the Government and its authorized representatives have unrestricted right to reproduce in whole or in part said article under any copyright owned by the publisher.

The Los Alamos Scientific Laboratory requests that the publisher identify this article as work performed under the auspices of the USERDA.



Los Alamos Scientific Laboratory  
of the University of California  
LOS ALAMOS, NEW MEXICO 87545

Anti-Discriminative Action/Equal Opportunity Employer

NOTICE  
This report was prepared as an account of work sponsored by the United States Government. Neither the United States nor the United States Energy Research and Development Administration, nor any of their employees, nor any of their contractors, subcontractors, or their employees, make any warranty, express or implied, or assume any legal liability or responsibility for the accuracy, completeness, or usefulness of any information, apparatus, product or process disclosed, or represent that its use would not infringe privately owned rights.

UNITED STATES  
ENERGY RESEARCH AND  
DEVELOPMENT ADMINISTRATION  
CENTRAL FILE ENG 36

MASTER

DISTRIBUTION OF THIS DOCUMENT IS UNLIMITED

## SOUND VELOCITY ON $\text{SiO}_2$ HUGONIOTS

J. A. Morgan and J. N. Fritz  
Los Alamos Scientific Laboratory  
Los Alamos, New Mexico

### INTRODUCTION

Silicon dioxide, with its phases having such widely differing densities and with its complex elastic-plastic behavior, is a fascinating material for high-pressure experimentation. Because it is a major constituent of the earth's mantle an added interest is given to data on  $\text{SiO}_2$  in pressure and temperature ranges that match those occurring in the mantle. The pioneering work of Wackerle [1] mapped out the response of  $\text{SiO}_2$  to initial loading. Much work has been done since then. Recently, emphasis has been on examining the properties of the high-pressure state by means of release waves and thermal radiation. Grady et al. [2,3] used overtaking release waves to study the bulk release wave in the pressure range 22-36 GPa. McQueen et al. [4] used thermal radiation from the high-pressure state to study pressure-temperature variation along the Hugoniot.

In this note we report measurements of release wave velocities in various samples of  $\text{SiO}_2$  shocked into the pressure range 47-67 GPa. We report on the first direct observation of a longitudinal release wave in  $\text{SiO}_2$  at these high pressures. The resulting sound speed data along the Hugoniot, combined with the Hugoniot, permit a calculation of the Grüneisen parameter along the Hugoniot. Because the pressure-temperature region of our experiments approximates middle mantle conditions, our longitudinal

and bulk velocity measurements for  $\text{SiO}_2$  have immediate implications for composition constraints to fit seismic profiles of sound velocities.

#### METHOD

The measurements which are described below employ a device called the Axially-Symmetric Magnetic (ASM) probe. [5] This device allows continuous measurement of the velocity of a highly-conducting plane surface. Figure 1 is a sketch of the experimental set-up illustrating the use of the probe. When the accelerating-reservoir light-gas (ARLG) gun (1) is fired an impactor disk of 2024 aluminum 6.35-mm-thick by 28-mm-diameter (2) is driven into a 3-mm-thick  $\text{SiO}_2$  target disk (3). An emf is induced in the pick-up coil (4) as a result of the motion of the aluminum impactor altering the field initially provided by the permanent magnet (5). A 75-nm-thick aluminum coating (6) is applied to the free surface of the  $\text{SiO}_2$  disk. This coating is too thin to affect the motion of the magnetic field (and thus the pick-up coil emf) except briefly while it is accelerated by the shock wave as it arrives at the  $\text{SiO}_2$  free surface. The emf produced in the pick-up coil by the motion of the surface of the aluminum disk is recorded by an oscilloscope onto film.

In the multiple-gage technique used by Grady et al. [2,3] a catch-up release wave is allowed to enter through the impactor system or a Taylor wave from a high explosive system is used. In contrast, in the present work the release wave originates at the free surface of the  $\text{SiO}_2$  disk. Because we effectively have only a single gage, we cannot use the powerful analysis given by Fowles and Williams [6] and Cowperthwaite and Williams. [7] However, in the high-pressure region where we are working, where the elastic wave, transition wave, and remaining pressure

increase are all a single discontinuity, the release wave emanating from the free surface is a simple wave. This makes possible an analysis of our data to obtain both longitudinal and bulk sound velocities as well as an estimate of the Hugoniot elastic limit at pressure. Figure 2 is one of the records obtained in experiment No. 103. We will use this to illustrate all our experiments. Several features of interest are indicated in the record. Region  $o'$  is the emf produced by the aluminum disk moving at constant velocity before impacting the  $SiO_2$  disk. At 1 impact occurs resulting in a lower velocity and an abrupt decrease in the emf. Note that the velocity of the aluminum surface after impact is the mass or particle velocity for both the silica and the aluminum. Region a is a record of the emf produced by that particle velocity. The tiny spike at 2 is due to the shock arrival at the  $SiO_2$  free surface as described above. Measurement of the time interval between features 1 and 2 and measurement of the thickness of the  $SiO_2$  disk before the experiment allow calculation of the shock velocity. The emf after feature 2 is still that due to the particle velocity although some electrical noise from the silica is apparent in this region. The features at 3 and 5 are arrival of the longitudinal and bulk release waves from the free surface at the  $SiO_2$ -aluminum interface. The emf due to interface velocity and thus the particle velocity associated with the longitudinal release is available from the record near feature 5. Careful attention to the details of the rarefaction arrival allow time interval measurements between features 2 and 3 and 5 to be made. These time intervals permit calculation of the sound velocities. Figure 3 is the velocity-time graph produced by analysis of the emf-time record shown in Fig. 2. The features  $o'$ , a, 1, 2, 3, and 5 indicated on this graph are a map of the correspondingly numbered features on the oscilloscope trace. The feature denoted c is explained below.

We relate the features described in the example experiment above to the Lagrangian  $y-t$  diagram shown in Fig. 4. In this diagram region  $o'$  is the state of the aluminum impactor before impact;  $o$  is the state of the  $SiO_2$  before passage of a shock wave; the region  $a$  denotes the state of both materials after passage of the initial shock wave; region  $b$  denotes that state resulting from the passage of a longitudinal release wave through state  $a$  in the  $SiO_2$ ; and region  $c$  denotes the state resulting from passage of a shock wave from interaction 3 through region  $b$ . Other features in this diagram are: 1 - impact of the aluminum onto the silica disk; 2 - arrival of the shock wave produced at 1 at the  $SiO_2$  free surface; 3 - arrival of the longitudinal release wave from the silica free surface at the aluminum- $SiO_2$  interface. From 3 a release wave propagates into the aluminum and a shock wave propagates back into the silica. This wave interacts with the bulk release wave at 4. The release wave from 4 to 5 passes through the state  $c$ .

$SiO_2$  disks in several forms were used. One experiment used fused silica, another used "gray novaculite" which contained about 6 wt% calcite and dolomite. Three experiments employed  $SiO_2$  in the form of "white novaculite" which had only a few ppm impurities. Finally two experiments used x-cut quartz single crystal disks. ARLG gun launch velocities varied from 4.7 km/s to 5.9 km/s.

#### RESULTS

From the particle velocity vs time record we obtain  $u_d$ , the impactor velocity;  $u_s$ , the shock velocity through the  $SiO_2$  sample;  $u_p$  ( $=u_a$ ), the particle velocity at the interface;  $c_L$ , the Lagrangian sound velocity of the longitudinal release wave;  $u_c$ , the particle velocity of the interface for state  $c$ , and  $c_B$ , the Lagrangian sound velocity of the bulk release wave.

Shock velocities were determined by using half-heights on the impact and pip portions of the curve; sound velocities were determined by using initial breaks in the curve. In addition termination of the recording indicating ASM probe destruction gave a rough indication of the free-surface velocity. We show the interactions and states (again with numbers appropriate to exp. no. 103) in the P-u plane in Fig. 5. (Incidentally, although we use the word pressure and the symbol P it will be recognized that we are really referring to normal stress.) The density and pressure at state a are obtained from the usual Hugoniot relations:  $P_a = \rho_0 u_s u_p$  and  $\rho_0 u_s = \rho_a (u_s - u_p)$ , where  $\rho_0$  is the initial density of the sample. The impactor velocity,  $u_d$ , and a known Hugoniot for the impactor:  $\rho_0 = 2.789 \text{ g/cm}^3$ ,  $c_0 = 5.328 \text{ km/s}$ ,  $s = 1.338$ ,  $\gamma_0 = 2.0$  with  $\partial E / \partial P)_V$  constant [8] - also give the pressure at the interface, viz.,  $P_{a \text{ Al}} = \rho_{a \text{ Al}} (u_d - u_p) [c_0 + s(u_d - u_p)]$ . We have shown these pressures as being coincident in Fig. 5. They will not be the same due to experimental error, but the agreement is quite satisfactory. The measurement of  $u_d$  is the weaker one because it comes from an early region in the record when the sensitivity is low. Because of experimental requirements a base line preliminary to the record was not obtained. We had to rely on the trace settling down to baseline after the pick-up coil was shorted. There was a slight uncertainty therefore ( $\sim 1-2\%$  of full signal) in the true zero voltage position. This slight shift causes the initial slope of the u-t record to vary considerably. Because the slope should be zero for this region we were able to "fine-tune" the position for zero voltage. This fine-tuning has no effect on timing and a very small effect on particle velocities in the later portion of the record when the signal is large.

Lagrangian sound velocities are simply the original sample thickness divided by the appropriate time interval. The true sound velocity at pressure can then be obtained from the relation:  $\rho c = \rho_0^x c$ . A first wave arrival is not obscured by secondary interactions. Our measurements of the velocity of longitudinal waves require no corrections and represent the wave velocity in state a. The bulk release, however, is propagating into state b (see Figs. 4 and 5). The longitudinal wave carries an appreciable pressure difference with it so we need to calculate the state b parameters. State b has been produced from state a by a longitudinal release up to incipient yielding. This state interacts with 2024 Al in state a. This results in a release in the aluminum and a shock in the  $\text{SiO}_2$  to state c. Because the  $\text{SiO}_2$  is going down and up the same path on a stress-strain curve it is reasonable to use the same absolute slope,  $\rho_0^x c_L$ , in the P-u plane for a **and b>c. From a measured  $u_c$  (see region c on Fig. 3) and a calculated impedance for 2024 aluminum,  $(\rho_0^x c_B)_{Al}$ , at state a, we get  $P_c$  from the relation:  $(P_c - P_a)/(u_c - u_a) = -(\rho_0^x c_B)_{Al}$ . (We use the bulk velocity for the aluminum although a longitudinal velocity might be somewhat more appropriate.) From the equality of the a **and b>c slopes we then get:  $2u_b = u_a + u_c + (P_a - P_c)/(\rho_0^x c_L)$  and  $2P_b = P_a + P_c - (\rho_0^x c_L)(u_c - u_a)$ . Applying the mass jump condition to the longitudinal release we obtain:  $\rho_a/\rho_b = 1 + (u_b - u_a)/c_L$ . A further correction to the value of  $c_B$  obtained should be made since the wave from Interaction 4 to 5 is traveling at  $c_L$ . For the present we ignore this correction because  $y_4 - y_5$  is much smaller than the sample thickness.****

The data for the individual experiments are presented in Table 1. There are a variety of materials and not all the experiments conform to the experimental arrangement we have described so far. In no. 75 the sample material was fused silica and a 0.23 mm 2024 aluminum plate was

glued to the back of the sample, i.e., between the impactor and the fused silica. We expected to measure a base line,  $u_p$ ,  $u_s$  and  $\epsilon_c$ . However the field trapped between the impactor and the shim somehow spilled through and ruined the  $u_p$  measurement. We used the data of McQueen et al. [4] for fused silica to infer  $u_p$ ,  $P_a$ , and  $\rho_a$  from  $u_s$ . No. 97 was a standard experiment but the  $\alpha$ -quartz sample was insufficiently electrically shielded. When the shock emerged from the free surface the noise generated by the piezoelectric crystal completely destroyed the ASM probe signal. We only obtained  $u_d$ ,  $u_s$  and  $u_p$  in this experiment. Subsequent samples have been coated with a 75 nm layer of aluminum to quiet this effect. In no. 108 some noise still manages to get through. The rest of the experiments had the standard arrangement. Nos. 105 and 107, our highest pressure shots, may have suffered from a lack of recording time. This is controlled by the spacing between the free surface and the ASM probe. We are not certain what the nature of the signal traces at the end of nos. 105 and 107 are. They may be release wave arrivals as we planned or they may be impact of the silica free surface into the ASM probe as we suspect. Only further experimentation will provide the answer.

For experiments nos. 103 and 108 we can do the analyses for the following bulk wave. These results are given in Table II.

Our Hugoniot data in the  $u_s$ - $u_p$  plane is shown in Fig. 6. We have also shown the data points obtained by Wackerle [1] and Trunin, et al. [9] that occur in the region represented. The linear fits to the data obtained by McQueen, et al. [4] are also shown. The sound velocities we obtained and those measured by Grady et al. [3] are shown in Fig. 7. Also indicated are the results from the ultrasonic work on stishovite



at zero pressure by Mitzutani et al. [10] and by Liebermann et al. [11], and the result of Olinger [12] from static high-pressure x-ray measurements.

#### DISCUSSION

Our Hugoniot data lies higher, in a systematic way and outside of experimental error, than the data of others. The film on the front of our sample will record the earliest arrival of any signal while flash-gap and pin data usually require a finite motion of the free surface to record a wave arrival. This would lead to a higher measured  $u_s$  in our experiments if there were some small precursor in front of the main wave. Indeed, there are later "bumps" in some of the records which, if taken to be indicative of a wave arrival, yield fair agreement with the flash-gap data. However, this shortens the time interval for release-wave travel and leads to unacceptably high values for the sound velocities. We are, at the moment, at a loss to explain this discrepancy. Our data are internally consistent, as shown by the agreement between pressures obtained from the direct  $u_s - u_p$  measurements and the pressure inferred from the  $u_p$  measurement and the equation of state for 2024 aluminum.

The sound velocities we have obtained are in reasonable agreement with the calculation of Grady et al. [3] and their highest experimental point. This point lies higher than ours as it would if it had any dispersive longitudinal component, however, the two points agree within the combined experimental error.

We have obtained evidence for separation of the release wave into a longitudinal and a bulk component. It is interesting that this

occurred most clearly in our sample which had a 6 wt% carbonate impurity. This could be because this sample produced less electrical noise and permitted us to identify these features in the record better, or it could be that the carbonate cement around quartz grains arrangement permitted an arrival at a final shocked state where the silica (now stishovite) grains had not been subjected to the shearing and layer melting postulated by Grady et al. [3]. However, we have also seen the wave separation on a quartz sample. All our samples were hit hard enough to effect a complete conversion to the high-pressure phase. The higher impact produces yielding on a finer scale. If the impact was sufficiently strong then individual dislocations could be nucleated and moved. Heterogeneous yielding in the lower pressure region and homogeneous yielding in our pressure region could explain why we see wave separation and Grady et al. do not. As the thermal energy deposited through this homogeneous yielding increases with increasing pressure we would expect the amplitude of the longitudinal wave to diminish and eventually disappear when melting occurs. The bulk wave we have measured, with the exception of the one in fused silica, does not in fact give us a true  $c_B(P)$ . This wave is propagating into a material whose normal stress has been relieved by a relatively large amount (10.6 GPa in no. 103 and 6.5 GPa in no. 108). The transverse stress will have gone down, but not by as much. Thus the wave is traveling into a non-hydrostatic state. Some corrections need to be made to infer the usual low amplitude quantities in  $c_B^2 = c_L^2 - (4/3)c_S^2$ . We shall not make them here in this short note. If the state prepared by the initial shock wave approximates a hydrostatic state, as we think it does in this case, then the stress decrease carried by the longitudinal wave is proportional to the Hugoniot elastic limit at this high pressure.

If we ignore the high values for  $c$  from no. 105 and 107 and extrapolate the trends shown in  $c_L$  and  $c_B$  we see that the longitudinal component vanishes at about 70 GPa. This roughly coincides with the transition found by McQueen et al. [4] with their pressure-temperature measurements. From their data the temperature at this pressure would be about 4200 K. Also from their data the temperatures of our experiments lie in the range 2000 - 3000 K (the temperature of the fused silica in experiment no. 75 is about 4000 K). The transition found by McQueen et al. could be either an anomalous melting transition or a transition to another solid phase. On the other hand if we do not discount the data from 105 and 107 (these give exceedingly high values, whether they be longitudinal or bulk) and if we interpreted these data as  $c_B$  values, then we would have a rapidly increasing  $c_B(P)$  and a vanishing  $c_L$  at about 60 GPa. The conclusion in this case would be that probably melting or perhaps a solid-solid phase transition occurred at about 60 GPa.

We have presented results from a variety of samples and treated the results as though they were all the same material. In the high pressure region each of the samples does go to the same phase although they vary in temperature at a given pressure because of a different initial density. Subtle differences show, and complete curves for a given sample type will be obtained. The electrical quietness of the "gray" Novaculite should be exploited. We have not yet gone to the upper limit of pressure attainable with this technique. By using a thinner sample and a warhead of higher impedance, having a larger spacing between sample and probe and thus a larger window for viewing the release wave, and paying some cost in time resolution we expect to extend these data up to 125 GPa.

## NOMENCLATURE

$y, t$	Lagrangian space coordinate, time
$\alpha, \alpha', a, b, c$	thermo- and hydrodynamic-states
$u_d$	impactor velocity
$u_p, u_a, u_b, u_c$	particle velocity
$u_s$	shock velocity
$z_c$	Lagrangian velocity
$c_L, c_B, c_S$	longitudinal, bulk, and shear wave velocities
$\rho_0, \rho$	initial density, density
$P$	pressure (normal stress)
$c_0, s$	linear $u_s - u_p$ Hugoniot parameters
$\gamma_0$	Grüneisen gamma

## REFERENCES

1. J. Wackerle, J. Appl. Phys., 33:922 (1962).
2. D. E. Grady, W. J. Murri, and G. R. Fowles, J. Geophys. Res., 79:332 (1974).
3. D. E. Grady, W. J. Murri, and P. S. DeCarli, J. Geophys. Res., 80:4857 (1975).
4. R. G. McQueen, J. N. Fritz, and J. W. Hopson, private comm., work to be published in near future.
5. J. N. Fritz and J. A. Morgan, Rev. Sci. Instrum., 44:215 (1973).
6. G. R. Fowles and R. F. Williams, J. Appl. Phys., 41:360 (1970).
7. M. Cowperthwaite and R. F. Williams, J. Appl. Phys., 42:456 (1971).
8. R. G. McQueen, S. P. Marsh, J. W. Taylor, J. N. Fritz and W. A. Carter, In High Velocity Impact Phenomena, ed. R. Kinslow, Academic Press, New York, p. 293 (1970).
9. R. F. Trunin, G. V. Sumakov, M. A. Podurets, B. N. Moiseyev, and L. V. Popov, 1970, Isv. Earth Phys. Ser., p. 13-20, March (Eng. Trans., same title, 1, 8-12 (1971)).
10. H. Mizutani, Y. Hamano, and S. Akimoto, J. Geophys. Res., 77:3744 (1972).
11. R. C. Liebermann, A. E. Ringwood, and A. Major, Earth Planet. Sci. Lett. (1977).
12. B. Olinger In High-Pressure Research, Applications In Geophysics, ed., M. H. Manghni and S. Akimoto, Academic Press. p.335 (1977).

**Table 1. Velocities and Derived Values from Impact Experiments**

exp. no./ materials <sup>a</sup>	$u_d$	$u_s$	$u_p$	$k_{c_L}$	$P_a$	$P_{a,Al}$	$\rho$	$c_L$
		km/s				GPa	g/cm <sup>3</sup>	km/s
75/A	-	6.67 ±.15	3.47	23.0 <sup>b</sup> ±1.0	51.1	-	4.597	11.0 <sup>b</sup> ±.5
97/B	4.88 ±.15	6.68 ±.23	2.75 ±.14	-	48.7	48.4	4.508	-
103/C	4.74 ±.05	6.83 ±.06	2.63 ±.02	20.9 ±.3	47.7	47.8	4.320	12.9 ±.2
104/D	5.19 ±.05	7.26 ±.07	2.85 ±.01	21.0 ±.4	54.8	55.1	4.359	12.7 ±.3
105/D	5.86 ±.08	7.57 ±.10	3.25 ±.03	25.7 <sup>c</sup> ±.7	65.1	64.1	4.637	14.7 <sup>c</sup> ±.4
107/D	5.91 ±.10	7.88 ±.20	3.21 ±.03	26.3 <sup>c</sup> ±.2	66.8	67.3	4.456	15.6 <sup>c</sup> ±.6
108/B	5.31 ±.10	7.38 ±.20	2.88 ±.03	20.3 ±.3	56.4	52.2	4.348	12.4 ±.2

a. A - fused silica,  $\rho_0 = 2.205 \text{ g/cm}^3$ ; B - x-cut  $\alpha$ -quartz,  $\rho_0 = 2.650 \text{ g/cm}^3$ ; C - a gray Arkansas novaculite, with 6 wt% of calcite and dolomite as an impurity,  $\rho_0 = 2.655$ ; D - a white Arkansas novaculite, essentially pure fine grained  $\alpha$ -quartz,  $\rho_0 = 2.645 \text{ g/cm}^3$ .

b. The values in this column are first wave velocities. They are probably longitudinal arrival times except for no. 75, where it is probably a bulk wave.

c. These high values are suspect. The experimental traces were noisy and probe destruction may have occurred too early to permit a release wave to be detected.

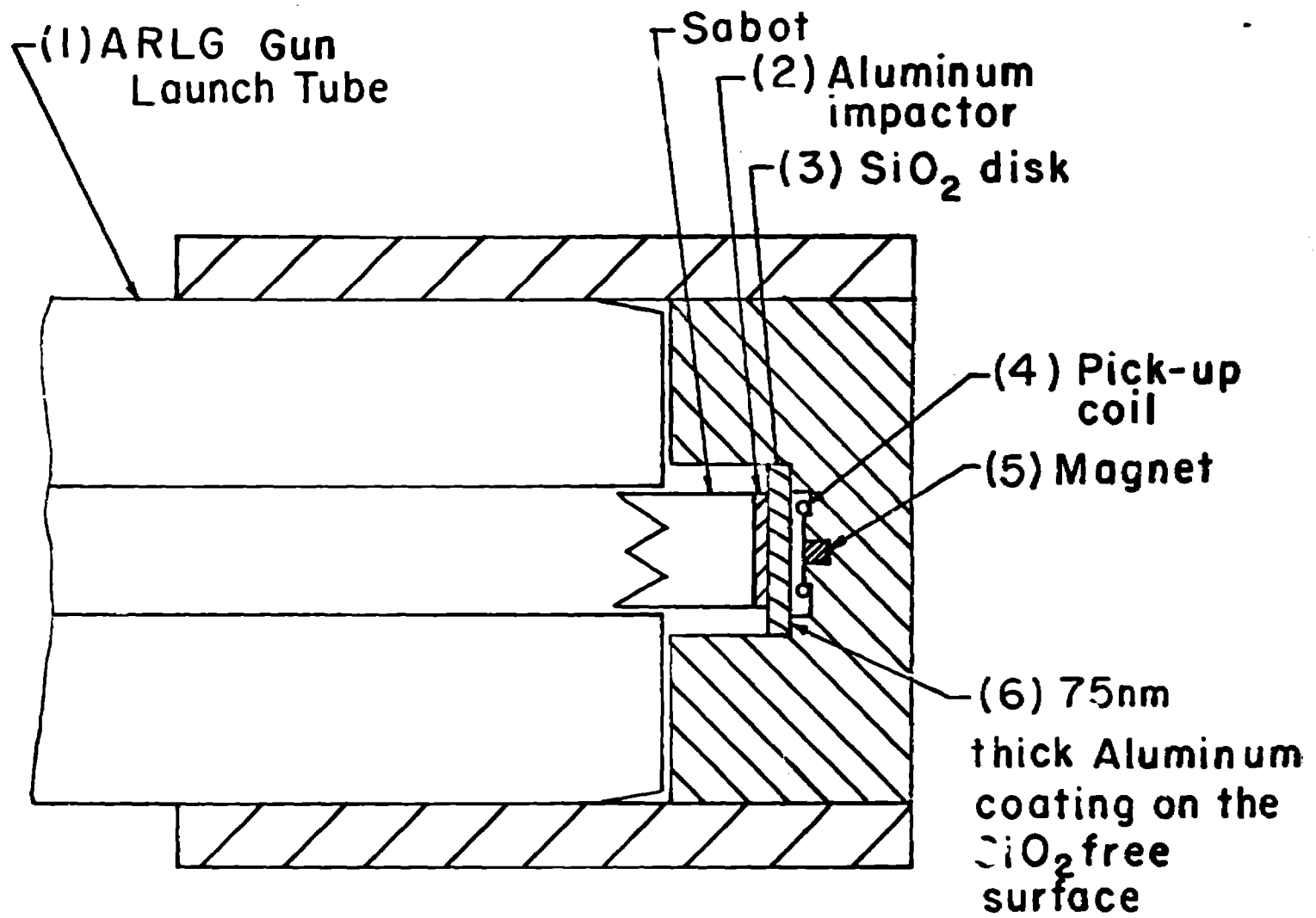
Table 11. Bulk velocities from No. 103 and 108

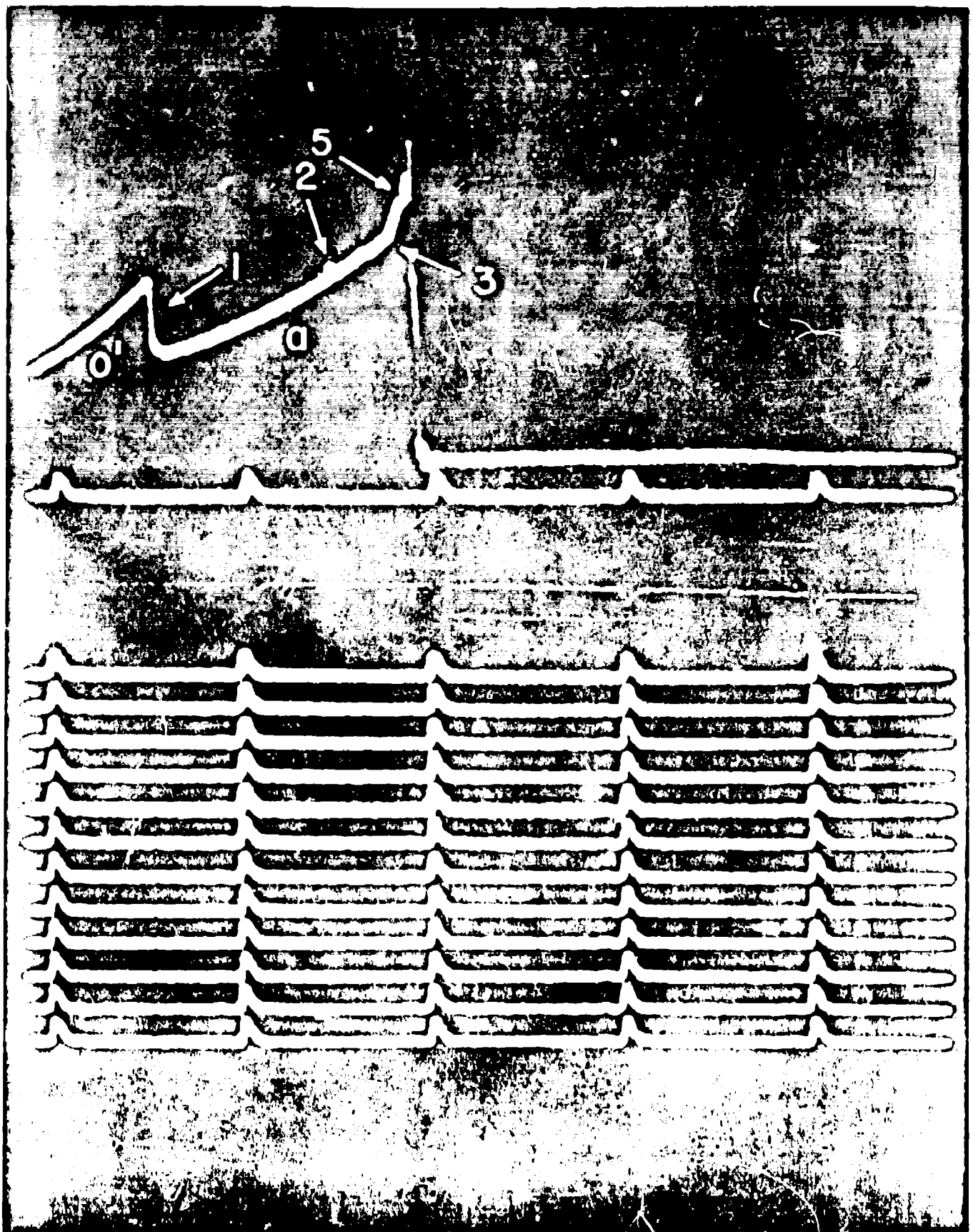
exp. no./ material	$u_c - u_a$ km/s	$\lambda_{cB}$	$P_c$ GPa	$u_b$ km/s	$\rho_b$ g/cm <sup>3</sup>	$P_b$ GPa	$c_B$ km/s	$P_a - P_b$ GPa
103/C	0.25	15.1	40.1	2.823	4.257	36.9	9.43	10.8
108/B	0.16	16.6	51.9	3.009	4.304	49.9	10.2	6.5

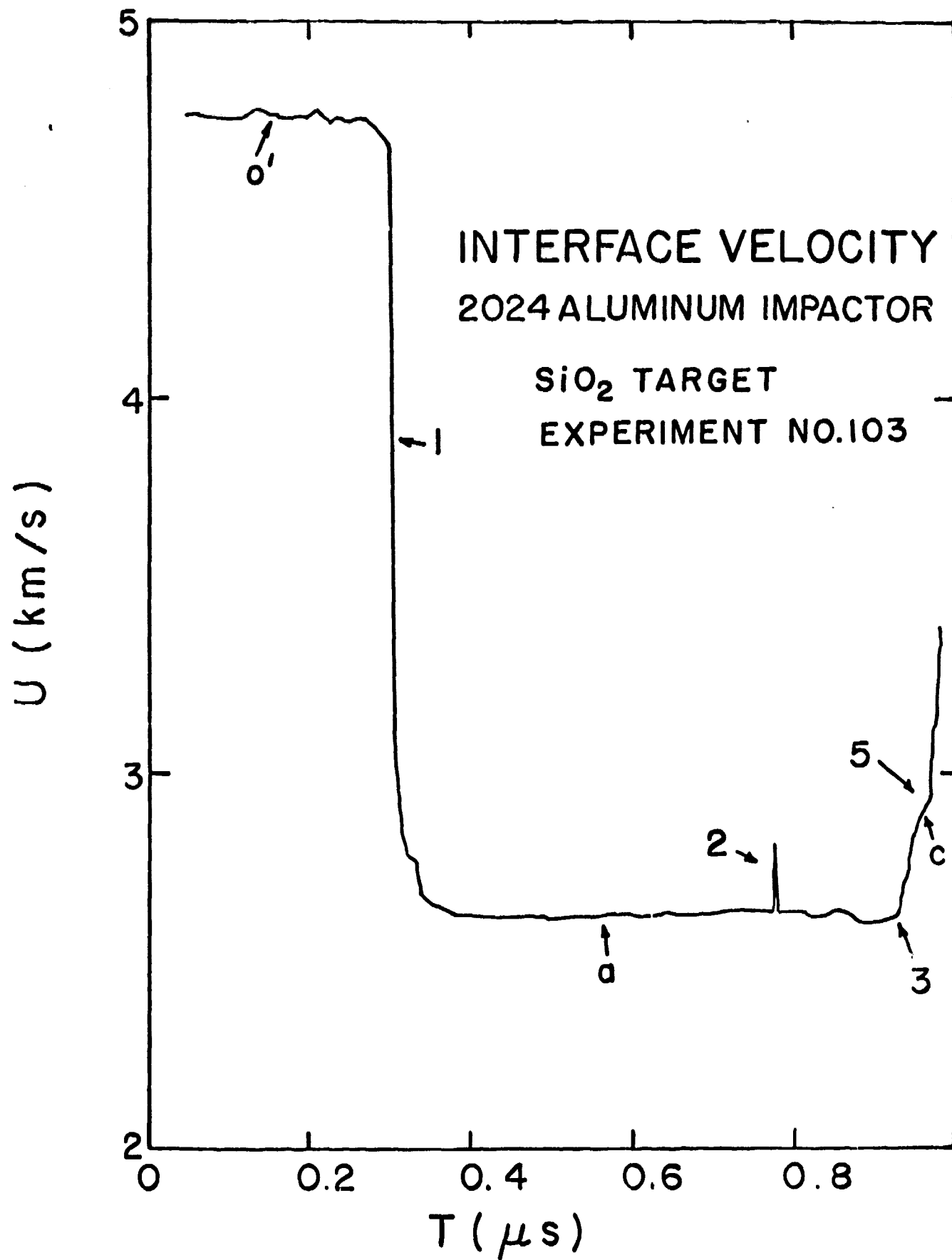
## FIGURE CAPTIONS

- Figure 1. ASM probe on ARLG gun, 2024 aluminum impactor on  $\text{SiO}_2$  target.
- Figure 2. Oscilloscope record of exp. no. 103, experimental trace and calibration grid.
- Figure 3. Reduced particle velocity vs. time, exp. no. 103
- Figure 4. Lagrangian y-t diagram, interactions and states in exp. no. 103.
- Figure 5. Pressure (normal stress) - particle-velocity representation of the interactions and states in exp. no. 103
- Figure 6.  $u_s - u_p$  Hugoniot curves for  $\text{SiO}_2$ .
- Figure 7. Sound velocities vs pressure for  $\text{SiO}_2$ .









why Y?

Y-T Diagram for Experiment No. 103

